


Spontaneous time-reversal symmetry breaking without magnetism in an $S = 1$ spin chain

Shun-Chiao Chang  and Pavan Hosur 

Texas Center for Superconductivity and Department of Physics, University of Houston, Houston, Texas 77204, USA

 (Received 11 November 2019; revised 4 September 2020; accepted 8 September 2020; published 4 November 2020)

States of matter that break time-reversal symmetry are invariably associated with magnetism or circulating currents. Recently, one of us proposed a phase, the directional scalar spin chiral order (DSSCO), as an exception: it breaks time-reversal symmetry via chiral ordering of spins along a particular direction, but is spin-rotation symmetric. In this work we prove the existence of this state via state-of-the-art density matrix renormalization group (DMRG) analysis on a spin-1 chain with nearest-neighbor bilinear-biquadratic interactions and additional third-neighbor ferromagnetic Heisenberg exchange. Despite the large entanglement introduced by the third-neighbor coupling, we are able to access system sizes up to $L = 918$ sites. We find first-order phase transitions from the DSSCO into the famous Haldane phase as well as a spin-quadrupolar phase where spin nematic correlations dominate. In the Haldane phase we demonstrate a method for detecting the topological edge states using DMRG that could be useful for other topological phases too. This method can be understood as the well-known active operators applied only at the boundary.

DOI: [10.1103/PhysRevB.102.174404](https://doi.org/10.1103/PhysRevB.102.174404)

I. INTRODUCTION

Equilibrium states of matter that break time-reversal symmetry (TRS) invariably contain a finite density of angular momentum, either spin or orbital. Common examples such as magnets contain local spin moments, while more complex ones include orbital moments, such as loop current phases [1,2], anomalous Hall states [3,4], and various chiral topological phases [5–14]. A property shared by these phases is that TRS is immediately restored when the moments melt. Thus, TRS breaking is usually considered synonymous with the formation of local moments, even though the latter also violate spatial symmetries of the lattice.

On the other hand, one of the authors recently proposed an exception to this rule, namely, the directional scalar spin chiral order (DSSCO) [15]. In one dimension, the DSSCO can be thought as a state in which quantum fluctuations have melted classical spin order in accordance with the Mermin-Wagner-Hohenberg-Coleman (MWHC) theorem [16–18] and restored SU(2) spin-rotation symmetry (SRS), but a vestigial scalar spin-chiral order captured by the order parameter

$$\chi = \frac{1}{L} \sum_i \langle \mathbf{S}_i \cdot (\mathbf{S}_{i+1} \times \mathbf{S}_{i+2}) \rangle, \quad (1)$$

where \mathbf{S}_i is the spin on the i th site, has survived. Since $\mathbf{S} \rightarrow -\mathbf{S}$ under time reversal, χ is an Ising order parameter that breaks TRS, but preserves SRS. It is reminiscent of some other phases that involve scalar spin chirality [19,20] such as chiral spin liquid [21]. The key difference is that the chirally correlated spins in all these examples lie on the vertices of a triangle. Hence, they break enough spatial symmetries to permit a moment perpendicular to its face, even if the on-site moment vanishes. In contrast, the corresponding sites in the DSSCO are on a straight line, so no such current is possible.

However, such current is possible in other scalar chiral phases based on ladders and two-dimensional (2D) lattices [22–34]. It also differs from phases with vector spin chirality [35], which preserves TRS but breaks SRS. Higher dimensional versions of the DSSCO rely on thermal or disorder-driven fluctuations for the restoration of SRS, with the latter proposed to be pertinent to the long-standing problem of the pseudogap phase of the cuprate superconductors, which show TRS breaking in Kerr effect measurements [36–39] but no signs of magnetism in nuclear magnetic resonance [40].

Reference [15] presented the DSSCO as a phase that is allowed by fundamental laws of quantum mechanics. However, it did not prove its existence in a realistic model. Through large-scale density matrix renormalization group (DMRG) analysis of a spin-1 chain, we fill this gap in knowledge by showing that the following spin-1 chain has the DSSCO as its ground state in a wide regime of parameters:

$$H = \sum_i K [\cos \theta (\mathbf{S}_i \cdot \mathbf{S}_{i+1})^2 + \sin \theta \mathbf{S}_i \cdot \mathbf{S}_{i+1}] - J \mathbf{S}_i \cdot \mathbf{S}_{i+3}. \quad (2)$$

Here $J, K > 0$ and $\theta \in [0, \pi/2]$ parametrizes the relative strengths of the bilinear and the biquadratic nearest-neighbor couplings. When $J = 0$, H reduces to the bilinear-biquadratic model that was studied in Ref. [41] and shown to realize a quasi-long-range ordered spin-quadrupolar (SQ) phase for $0 < \theta < \pi/4$ and the Haldane phase $\theta > \pi/4$, separated by a Berezinskii-Kosterlitz-Thouless type phase transition at $\theta = \pi/4$ [42]. We explore the effects of nonzero J on this model and find that the SQ is driven into the DSSCO, either directly or via intermediate Haldane and disordered phases, while the Haldane phase simply disorders at finite J for most values of θ . In the $J \rightarrow \infty$ limit, H reduces to three copies of a

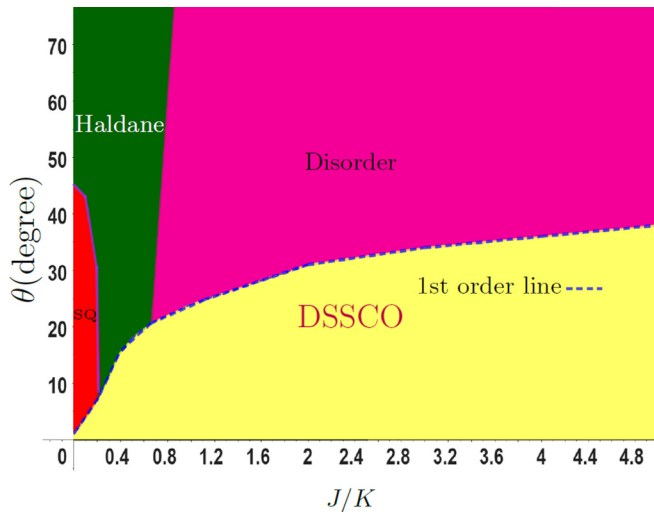


FIG. 1. The ground state phase diagram of the spin-1 Hamiltonian in (2). The DSSCO, Haldane, spin-quadrupolar (SQ) and disordered phases are identified. Dotted lines denote first-order phase transitions between the DSSCO and the other three phases.

Heisenberg ferromagnet, while finite J introduces quantum fluctuations that melt the ferromagnet in accordance with the MWHC theorem [16–18]. The full phase diagram is shown in Fig. 1.

The emergence of the DSSCO as a ground state of H can be anticipated heuristically as follows. In the classical limit, $S \rightarrow \infty$, the biquadratic term $K \cos \theta$ dominates and forces adjacent spins to be mutually orthogonal. At $\theta = 0$, the remaining ferromagnetic coupling J favors parallel third neighbors, resulting in two degenerate ground state manifolds $R|x, y, z, x, y, z, \dots\rangle$ and $R|-x, -y, -z, -x, -y, -z, \dots\rangle$ that are related by time reversal and have opposite expectation values of χ . Above, $\pm x$ at the i th position in the ket denotes a state with spin at the i th site maximally polarized along $\pm x$ and $R \in \text{SU}(2)$ represents an arbitrary global spin rotation. The classical ground state is then randomly chosen from these manifolds, thus breaking TRS and SRS spontaneously. For finite S , quantum fluctuations produce smooth deformations in the magnetization texture or gapless spin waves. In one dimension, these fluctuations are strong enough to melt the underlying spin order and restore SRS [16–18]. However, smooth deformations cannot change the chirality of the ground state, thus yielding the DSSCO. In this work we find that the ground state at $\theta = 0$ is the boundary between ferromagnetic phase and DSSCO. A nonzero θ is needed to stabilize the DSSCO. However, a large θ again destabilizes it in favor of the Haldane or the disordered phase.

II. NUMERICAL PROCEDURE

We carry out state-of-the-art DMRG calculations using the ITensor library developed by Stoudenmire and White [43]. We perform up to 215 sweeps with a final maximum bond dimension of $m = 800$, which restricts the truncation error to below 10^{-6} . We are able to access system sizes up to $L = 918$ despite our model containing a third-nearest-neighbor interaction.

In comparison, DMRG calculations on the simpler bilinear-biquadratic spin-1 chain, which has only nearest-neighbor and next-nearest-neighbor terms, went only to $L = 300$ sites [44]. Such a dramatic improvement in the performance results from using a pinning field on open chains to diagnose the phases of interest. We elaborate on this technique below.

Naively, ordering is captured by the unbiased correlation function:

$$m = \lim_{L \rightarrow \infty} \sqrt{\frac{1}{L} \sum_i e^{iqi} \langle A_1 A_i \rangle_H}, \quad (3)$$

where A_i is an operator that corresponds to the order parameter on the i th site and H is the Hamiltonian whose ground state the expectation value is computed in. In the current problem we consider three choices of A_i : spin S_i^z , quadrupole Q_i^{zz} , and $\chi_i = \mathbf{S}_i \cdot (\mathbf{S}_{i+1} \times \mathbf{S}_{i+2})$. A finite value of m signals long-ranged order and spontaneous breaking of symmetry. However, this approach requires very large system sizes and high precision to obtain reliable results, since it computes the square of the local order parameter, which can be a very small, especially close to a phase boundary. This issue can be circumvented by adding a training field with an appropriate Fourier component $H' = h \sum_i e^{iqi} A_i$ to H and computing

$$m = \lim_{h \rightarrow 0} \lim_{L \rightarrow \infty} \frac{1}{L} \sum_i e^{iqi} \langle A_i \rangle_{H+h \sum_i e^{iqi} A_i}. \quad (4)$$

The ordering of limits is crucial: one first has to take the thermodynamic limit and then the limit of vanishing training field $h \rightarrow 0$. Such an approach was used, for instance, in Ref. [45].

We go a step further and consider a *local* field $H'' = h_1 A_1$ localized on the first site (or first three sites when $A_i = \chi_i$). This trick lifts the burden of taking $h \rightarrow 0$ numerically. In fact, we can make h_1 strong enough to saturate the order at the first site [46]. Then, long-range order is captured by

$$m = \lim_{i \rightarrow \infty} \lim_{L \rightarrow \infty} e^{iqi} \langle A_i^z \rangle_{H+h_1 A_1}. \quad (5)$$

That is, one first has to take the thermodynamic limit and then take the distance from the pinning center to infinity. This approach has been shown to be less sensitive to finite-size effects of the order parameter than the other two methods [47]. In following sections we will use this method to diagnose the spin and spin-quadrupolar orders. Applying it to the DSSCO, however, causes the code to get stuck in metastable states with fractionalized Ising domain wall excitations [48]. Therefore, we use Eq. (4) for DSSCO with $q = 0$ since a uniform field destabilizes the domain walls and helps find the true ground state.

Although the Hamiltonian has SRS and thus commutes with $S_{\text{total}}^z = \sum_i S_i^z$, we found that implementing DMRG separately within each S_{total}^z subspace resulted in significantly slower or sometimes no convergence. We speculate that this may be because fixing S_{total}^z to a nonzero value N amounts to an interaction $H_U = U(S_{\text{total}}^z - N)^2 = U \sum_{i,j} S_i^z S_j^z + 2NU \sum_i S_i^z + \text{const.}$, $U \rightarrow \infty$. This contains coupling between spins that are far apart, which would tend to slow down the DMRG calculation. Luckily, ordinary gapped phases have short-ranged spin correlations, so the slowdown

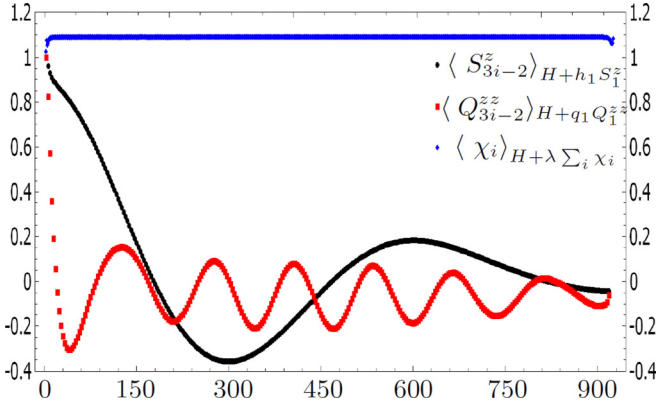


FIG. 2. Order parameters in the DSSCO phase measured by applying appropriate training fields. A weak uniform training chiral field $\lambda = 0.01$ is used to probe the chiral order, whereas spin and spin-quadrupolar correlations are probed by applying strong training fields $h_1 = q_1 = 50$ at the first site. The spin and spin-quadrupolar orders decay to zero over long distances, which suggests the absence of long-range order in these variables. Data shown are for $L = 918$ at $J/K = 1$ and $\theta = 20^\circ$.

and the net effect of this fixing S_{total}^z is to speed up the procedure by reducing the size of the Hilbert space. In the current problem, however, the range of spin-spin correlations is only limited by the MWHC theorem and hence is extremely large (as we also show below). Consequently, the speed-up because of a smaller Hilbert space cannot offset the slowdown due to the long-range coupling in H_U . Thus, in our implementation, we allow the program to explore different values of S_{total}^z while searching for the ground state.

III. RESULTS: PHASE DIAGRAM

Figure 1 summarizes the phase diagram of the Hamiltonian (2) obtained by DMRG. We reproduced known results on the bilinear-biquadratic model [41] for the spin quadrupolar and the Haldane phases on the $J = 0$ axis. For small negative θ and $J = 0$ the ground state is known to be ferromagnetic [41]. Unsurprisingly, we found (but do not show in Fig. 1) that the ferromagnet survives nonzero J . Interestingly, all the phases share boundaries with the DSSCO, which is the primary focus of this work.

A. DSSCO phase

The most exciting feature of the phase diagram is the DSSCO, which breaks TRS but preserves SRS. We show numerical evidence for this phase in Figs. 2 and 3. Computations of on-site $\langle \chi_i \rangle$ and chiral order χ shown in Figs. 2–4, and 7 adapt the method from (4) to the Hamiltonian (1) through the equation

$$\chi = \lim_{\lambda \rightarrow 0} \lim_{L \rightarrow \infty} \frac{1}{L} \sum_i \langle \chi_i \rangle_{H+\lambda \sum_i \chi_i}, \quad (6)$$

while computations of $\langle S_i^z \rangle$ and $\langle Q_i^{zz} \rangle$ use the method from (5).

Figure 2 shows that pinning the chirality of the first three sites induces chiral ordering of $O(1)$ magnitude throughout

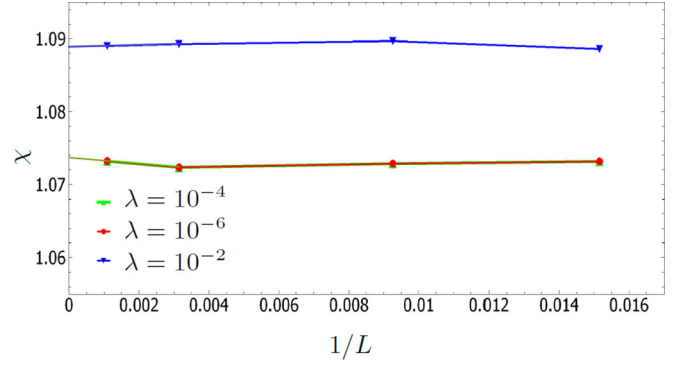


FIG. 3. Finite-size scaling of χ for multiple weak uniform training chiral fields at $J = 1$ and $\theta = 20^\circ$. Clearly χ survives as the training field is switched off, which indicates the formation of an ordered phase, namely, the DSSCO, via spontaneous symmetry breaking.

the chain. Moreover, as shown in Fig. 3, it robustly survives finite size scaling to the thermodynamic limit $L \rightarrow \infty$, even as the pinning field λ is tuned down. In contrast, Fig. 2 shows that spin and spin-quadrupolar orders decay to zero despite pinning their values on the first site. Note, $\langle S_i \rangle$ and $\langle \hat{Q}_i \rangle$ have been shown on every third site. This is because the classical magnetic order that the DSSCO emerges from induces $q = 2\pi/3$ oscillations in them that are not the subject of our interest; we are interested in the amplitude of these oscillations only. Thus, in accordance with the MWHC theorem [16–18] which allows (forbids) discrete (continuous) symmetry breaking in one dimension, the DSSCO breaks TRS and shows long-range order while spin and spin quadrupoles only show short-range order, since their order parameters break continuous SRS. The oscillations of spin and quadrupolar are macroscopic, with periods comparable to the system size. As J increases, the periods increase, and diverge in the limit $J \rightarrow \infty$ where the system reduces to three copies of the Heisenberg ferromagnet.

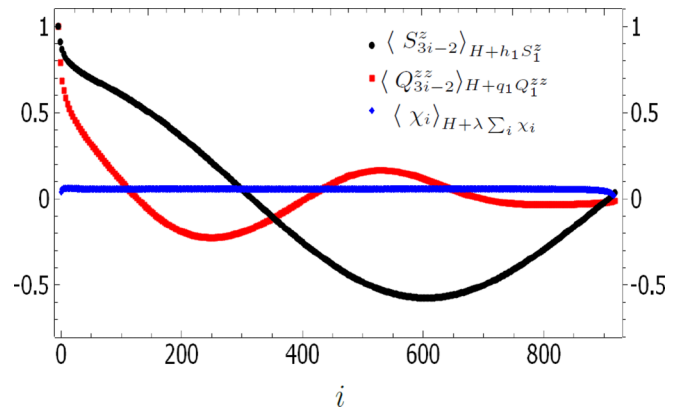


FIG. 4. Order parameters in the disorder phase measured by the same training fields in Fig. 2. The chiral order is nearly zero everywhere indicating the system has no response to weak uniform chiral field while the spin and spin-quadrupolar orders decay to zero over long distances, which suggests the absence of long-range order in these variables. Data shown are for $L = 918$ at $J/K = 1.3$ and $\theta = 45^\circ$.

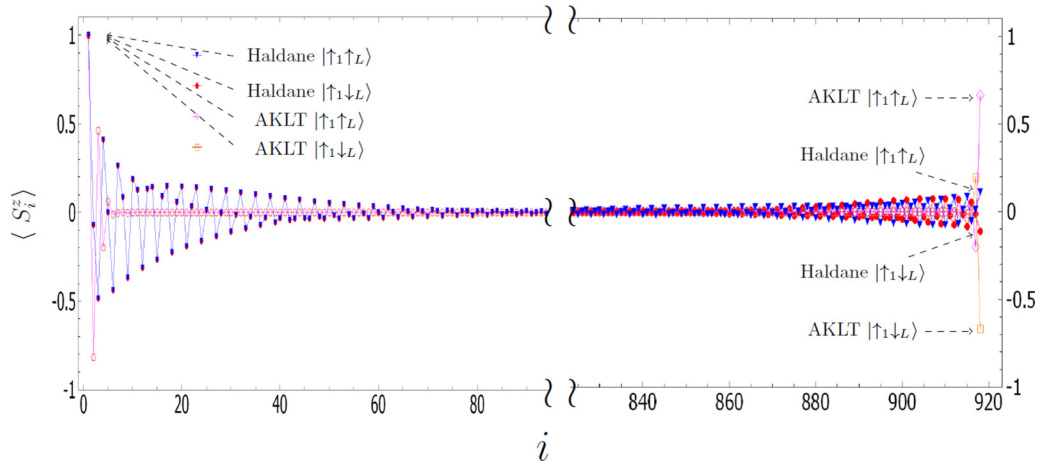


FIG. 5. Edge states in the Haldane phase. Two degenerate ground states for Haldane phases at $\theta = 15^\circ$, $J/K = 0.3$ and for AKLT point $\theta = 71.5^\circ$, $J = 0$ are shown and the spins on the edges are marked by dashed arrows. The moment at the first site is saturated by a local training field, and $\langle S_i^z \rangle$ is measured at all the sites. For each set of parameters $(\theta, J/K)$, $\langle S_i^z \rangle$ on the right edge is large while $\langle S_i^z \rangle$ in the bulk is extremely small. Note, bulk sites between $i \approx 100$ and $i \approx 820$ are not shown to highlight the edge states.

A plausible reason for the periods of spin and quadrupolar orders to be different is that the latter is a higher-order spin operator. However, this is difficult to verify with the current numerics because both orders have extremely large correlation lengths. Outside the DSSCO, χ vanishes in the Haldane, spin-quadrupolar, and disordered phases. In the disorder phase as in Fig. 4, based on the same training fields in Fig. 2, the chiral order vanishes indicating the system has no response to weak uniform chiral field while the spin and spin-quadrupolar orders decay to zero over long distances similar to DSSCO, which suggests the absence of long-range order in these variables.

In the following we will discuss spin order in the Haldane phase, where the bulk is naively disordered but a hidden order exists between the edges, as well as the spin-quadrupolar phase where either quasi-long-range order or disorder exists.

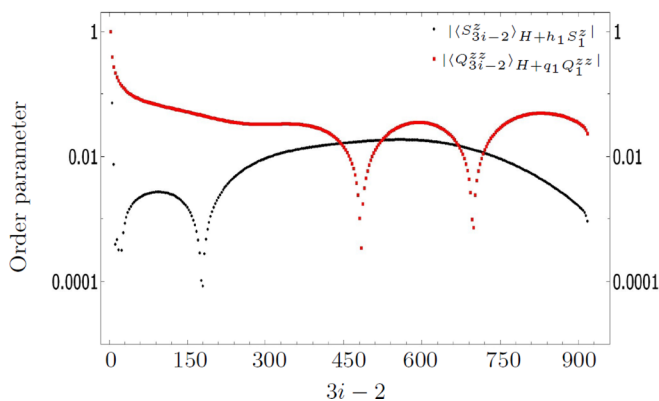


FIG. 6. Spin and spin-quadrupolar orders in the spin-quadrupolar phase, at $\theta = 5^\circ$ and $J/K = 0.1$, determined by measuring S^z and Q^{zz} on every third site after pinning S^z and Q^{zz} on the first site with large training fields $h_1 = 50$ and $q_1 = 50$, respectively. The system size is $L = 918$. Flattening of the curves for a broad range of sites suggest a large correlation length.

B. Pinning the Haldane phase

The Haldane phase is one of the simplest examples of a symmetry-protected topological phase [49–51]. Its simplest realization is in the antiferromagnetic Heisenberg model, which is the $\theta = \pi/2$, $J = 0$ limit of H , while the point $\theta = \tan^{-1} 3 \approx 71.5^\circ$, $J = 0$ is in the same phase and corresponds to the exactly soluble Affleck-Kennedy-Lieb-Tasaki (AKLT) point [52]. The Haldane phase has no local order parameter; instead, it can be characterized by a nonlocal string order parameter [53,54] that captures entanglement between states on opposite ends of the chain. In particular, the ground state in the Haldane phase is fourfold degenerate on an infinite open chain. The degeneracy stems from the two effective spin-1/2s, one exponentially localized at each end [54,55]. For a finite chain, the states at opposite ends hybridize, resulting in a unique singlet ground state: $\frac{1}{\sqrt{2}}(|\uparrow_1 \downarrow_L\rangle - |\downarrow_1 \uparrow_L\rangle)$, and a threefold-degenerate triplet of excited states: $|\uparrow_1 \uparrow_L\rangle$, $\frac{1}{\sqrt{2}}(|\uparrow_1 \downarrow_L\rangle + |\downarrow_1 \uparrow_L\rangle)$, and $|\downarrow_1 \downarrow_L\rangle$. In the thermodynamic limit the singlet and triplet sectors become exactly degenerate. Therefore, the edge states can be detected by directly computing spin-spin correlation function in the ground state using (3), which is equivalent to calculating the string order. The correlation is nontrivial between the opposite ends of the chain, but vanishes between an edge site and a bulk site.

We expect the Haldane phase to occur in our model as well in a region of phase space around the Heisenberg and AKLT points. However, the third-neighbor interactions increase the ground state entanglement, which drastically increases the cost of computing the nonlocal order. We therefore adopt an alternate strategy to detect the edge states that not only avoids measuring the nonlocal order but also reduces the entanglement of our ground state. We apply a spin-pinning field on the first site, which reduces the fourfold degenerate space to two doubly degenerate subspaces, $(|\uparrow_1 \uparrow_L\rangle, |\uparrow_1 \downarrow_L\rangle)$ and $(|\downarrow_1 \uparrow_L\rangle, |\downarrow_1 \downarrow_L\rangle)$, since the pinning field favors (disfavors) states with spin at the first site parallel (antiparallel) to the field. Figure 5 shows signatures of the edge states in

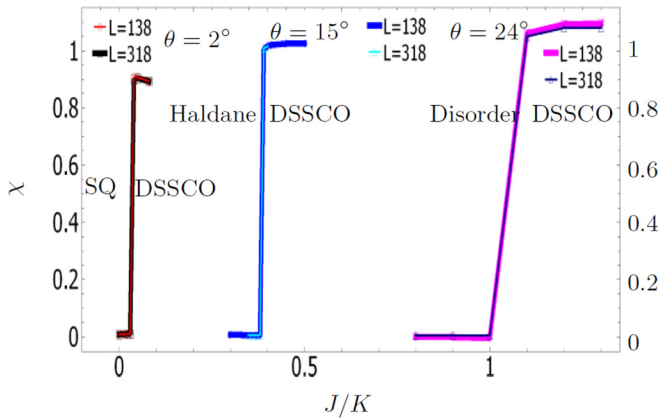


FIG. 7. Phase transitions out of the DSSCO phase into the disordered, Haldane, and spin-quadrupole phases for two different sizes L . The abrupt change in χ as well as the weak L dependence indicates the first-order phase transitions. Here uniform field $\lambda = 0.01$ is used to train χ .

the Haldane phase at $\theta = 15^\circ$, $J/K = 0.3$, and at the AKLT point [52]. The exactly soluble AKLT point shows sharp spin moments at the edges, whereas the moments elsewhere in the Haldane phase decay exponentially into the bulk.

Our method is in contrast to the trick used in the early days of DMRG to detect the Haldane phase, which involved artificial spin-1/2 degrees of freedom to the ends of the spin-1 chain to lift the fourfold degeneracy and achieve convergence [46,54]. It is more closely related to the idea of active operators [56], where a small field was added throughout the system to lift the ground state degeneracy resulting from edge states. Our approach involves a nonperturbative field only at the edges in DMRG to lift the degeneracy and is better suited for numerical implementation.

C. Spin-quadrupole phase

We apply pinning spin and spin-quadrupolar fields at the first site separately and measure spin and spin-quadrupolar orders, respectively, far away from pinning center and edges according to Eq. (5). Again, $q = 2\pi/3$ oscillations are removed by computing order parameters every three sites. The results are shown in Fig. 6. It shows that correlation length is

extremely large and possibly diverges. Reference [57] shows that the correlation length indeed diverges at $J = 0$, $0 < \theta < \pi/4$ and the dominant correlations are spin quadrupolar. At the systems sizes we can access, we are unable to determine decisively whether nonzero J induces a gapped phase with exponentially decaying spin-quadrupolar correlations with a large correlation length or a critical phase like the $J = 0$ limit. The resolution of this issue is left for future work.

D. Phase transitions out of the DSSCO

In Fig. 7 we show phase transitions from the DSSCO to the other phases which are disordered phase, Haldane phase, and spin-quadrupole phase by calculating chiral order χ using Eqs. (2) and (6). The abrupt drops in χ to zero clearly at the phase boundaries indicate first-order phase transitions. Another indication of first-order transitions is the weak dependence of χ on the system size. Since the correlation length does not diverge at the critical point for first-order phase transitions, boundary effects are small, which result in a weak system-size dependence. Similar ideas were used to diagnose first-order phase transitions in Ref. [44].

IV. CONCLUSIONS

The DSSCO is a novel phase of matter that violates TRS but has no density of moments, unlike other TRS-breaking phases known in condensed matter. Using DMRG, we find that it appears when spin and quadrupolar orders melt, leaving behind residual broken TRS but unbroken continuous SRS. The chiral order is $O(1)$ in the DSSCO, which is much larger than that in other existing chiral phases such as the chiral spin liquid, where $\chi \sim O(10^{-1})$ [21]. Besides, we demonstrate a numerical method to study edge states by pinning one edge and observing the other. It would be interesting to study other one-dimensional topological phases using this method.

ACKNOWLEDGMENTS

We would like to Miles Stoudenmire and Yixuan Huang for invaluable discussions. We acknowledge the Department of Physics and the College of Natural Sciences and Mathematics and the Robert A. Welch Foundation Grants No. E-1146 and No. E-1070 (S.C.) for financial support.

-
- [1] C. M. Varma, *Phys. Rev. B* **55**, 14554 (1997).
 - [2] Y. He and C. M. Varma, *Phys. Rev. B* **86**, 035124 (2012).
 - [3] F. D. M. Haldane, *Phys. Rev. Lett.* **61**, 2015 (1988).
 - [4] N. Nagaosa, J. Sinova, S. Onoda, A. H. MacDonald, and N. P. Ong, *Rev. Mod. Phys.* **82**, 1539 (2010).
 - [5] V. Kalmeyer and R. B. Laughlin, *Phys. Rev. Lett.* **59**, 2095 (1987).
 - [6] H. Yao and S. A. Kivelson, *Phys. Rev. Lett.* **99**, 247203 (2007).
 - [7] X. G. Wen, F. Wilczek, and A. Zee, *Phys. Rev. B* **39**, 11413 (1989).
 - [8] A. Dhar, T. Mishra, M. Maji, R. V. Pai, S. Mukerjee, and A. Paramekanti, *Phys. Rev. B* **87**, 174501 (2013).
 - [9] M. P. Zaletel, S. A. Parameswaran, A. Rüegg, and E. Altman, *Phys. Rev. B* **89**, 155142 (2014).
 - [10] C. Kallin and A. J. Berlinsky, *J. Phys.: Condens. Matter* **21**, 164210 (2009).
 - [11] A. J. Leggett, *Rev. Mod. Phys.* **47**, 331 (1975).
 - [12] D. D. Osheroff, R. C. Richardson, and D. M. Lee, *Phys. Rev. Lett.* **28**, 885 (1972).
 - [13] D. D. Osheroff, W. J. Gully, R. C. Richardson, and D. M. Lee, *Phys. Rev. Lett.* **29**, 920 (1972).
 - [14] A. Tsuruta, S. Yukawa, and K. Miyake, *J. Phys. Soc. Jpn.* **84**, 094712 (2015).
 - [15] P. R. Hosur, *J. Phys.: Condens. Matter* **32**, 255604 (2020).
 - [16] N. D. Mermin and H. Wagner, *Phys. Rev. Lett.* **17**, 1133 (1966).

- [17] P. C. Hohenberg, *Phys. Rev.* **158**, 383 (1967).
- [18] S. Coleman, *Commun. Math. Phys.* **31**, 259 (1973).
- [19] D. Grohol, K. Matan, J.-H. Cho, S.-H. Lee, J. W. Lynn, D. G. Nocera, and Y. S. Lee, *Nat. Mater.* **4**, 323 (2005).
- [20] P. A. Lee and N. Nagaosa, *Phys. Rev. B* **87**, 064423 (2013).
- [21] S.-S. Gong, W. Zhu, J.-X. Zhu, D. N. Sheng, and K. Yang, *Phys. Rev. B* **96**, 075116 (2017).
- [22] T. Momoi, T. Hikihara, M. Nakamura, and X. Hu, *Phys. Rev. B* **67**, 174410 (2003).
- [23] S. Taira, C. Yasuda, T. Momoi, and K. Kubo, *J. Phys. Soc. Jpn.* **88**, 014701 (2019).
- [24] K. Okunishi, M. Sato, T. Sakai, K. Okamoto, and C. Itoi, *Phys. Rev. B* **85**, 054416 (2012).
- [25] P. Lecheminant and K. Totsuka, *Phys. Rev. B* **71**, 020407(R) (2005).
- [26] L. N. Bulaevskii, C. D. Batista, M. V. Mostovoy, and D. I. Khomskii, *Phys. Rev. B* **78**, 024402 (2008).
- [27] D. I. Khomskii, *J. Phys.: Condens. Matter* **22**, 164209 (2010).
- [28] G. Gorohovsky, R. G. Pereira, and E. Sela, *Phys. Rev. B* **91**, 245139 (2015).
- [29] T. Hikihara, T. Momoi, and X. Hu, *Phys. Rev. Lett.* **90**, 087204 (2003).
- [30] A. Läuchli, G. Schmid, and M. Troyer, *Phys. Rev. B* **67**, 100409(R) (2003).
- [31] M. Sato, *Phys. Rev. B* **76**, 054427 (2007).
- [32] K. A. Al-Hassanieh, C. D. Batista, G. Ortiz, and L. N. Bulaevskii, *Phys. Rev. Lett.* **103**, 216402 (2009).
- [33] A. Kolezhuk and T. Vekua, *Phys. Rev. B* **72**, 094424 (2005).
- [34] C. D. Batista, *Phys. Rev. B* **80**, 180406(R) (2009).
- [35] S. R. Manmana, A. M. Läuchli, F. H. L. Essler, and F. Mila, *Phys. Rev. B* **83**, 184433 (2011).
- [36] J. Xia, E. Schemm, G. Deutscher, S. A. Kivelson, D. A. Bonn, W. N. Hardy, R. Liang, W. Siemons, G. Koster, M. M. Fejer, and A. Kapitulnik, *Phys. Rev. Lett.* **100**, 127002 (2008).
- [37] S. Spielman, J. S. Dodge, L. W. Lombardo, C. B. Eom, M. M. Fejer, T. H. Geballe, and A. Kapitulnik, *Phys. Rev. Lett.* **68**, 3472 (1992).
- [38] S. Spielman, K. Fesler, C. B. Eom, T. H. Geballe, M. M. Fejer, and A. Kapitulnik, *Phys. Rev. Lett.* **65**, 123 (1990).
- [39] H. Karapetyan, J. Xia, M. Hücker, G. D. Gu, J. M. Tranquada, M. M. Fejer, and A. Kapitulnik, *Phys. Rev. Lett.* **112**, 047003 (2014).
- [40] T. Wu, H. Mayaffre, S. Krämer, M. Horvatić, C. Berthier, W. N. Hardy, R. Liang, D. A. Bonn, and M.-H. Julien, *Nat. Commun.* **6**, 6438 (2015).
- [41] Y.-T. Oh, H. Katsura, H.-Y. Lee, and J. H. Han, *Phys. Rev. B* **96**, 165126 (2017).
- [42] C. Itoi and M.-H. Kato, *Phys. Rev. B* **55**, 8295 (1997).
- [43] E. M. Stoudenmire and S. R. W. White, Itensor, <http://itensor.org>.
- [44] P. Corboz, A. M. Läuchli, K. Totsuka, and H. Tsunetsugu, *Phys. Rev. B* **76**, 220404(R) (2007).
- [45] M. V. Ulybyshev, P. V. Buividovich, M. I. Katsnelson, and M. I. Polikarpov, *Phys. Rev. Lett.* **111**, 056801 (2013).
- [46] S. R. White and A. L. Chernyshev, *Phys. Rev. Lett.* **99**, 127004 (2007).
- [47] F. F. Assaad and I. F. Herbut, *Phys. Rev. X* **3**, 031010 (2013).
- [48] P. Prelovšek and I. Sega, *Phys. Lett. A* **81**, 407 (1981).
- [49] F. D. M. Haldane, *Phys. Lett. A* **93**, 464 (1983).
- [50] F. D. M. Haldane, *Phys. Lett. Lett.* **50**, 1153 (1983).
- [51] F. Pollmann, E. Berg, A. M. Turner, and M. Oshikawa, *Phys. Rev. B* **85**, 075125 (2012).
- [52] I. Affleck, T. Kennedy, E. H. Lieb, and H. Tasaki, *Phys. Rev. Lett.* **59**, 799 (1987).
- [53] H. Ueda, H. Nakano, and K. Kusakabe, *Phys. Rev. B* **78**, 224402 (2008).
- [54] S. R. White and D. A. Huse, *Phys. Rev. B* **48**, 3844 (1993).
- [55] T. Kennedy, *J. Phys.: Condens. Matter* **2**, 5737 (1990).
- [56] Z.-X. Liu, Z.-B. Yang, Y.-J. Han, W. Yi, and X.-G. Wen, *Phys. Rev. B* **86**, 195122 (2012).
- [57] A. Läuchli, G. Schmid, and S. Trebst, *Phys. Rev. B* **74**, 144426 (2006).